INORGANIC CHEMISTRY
FRONTIERS

RESEARCH ARTICLE

View Article Online
View Journal | View Issue

Cite this: *Inorg. Chem. Front.*, 2019, **6**, 1405

Field-induced slow relaxation of magnetization in the *S* = 3/2 octahedral complexes *trans*-[Co{(OPPh$_2$)(EPPh$_2$)N}$_2$(dmf)$_2$], E = S, Se: effects of Co–Se *vs.* Co–S coordination†

Eleftherios Ferentinos,‡[a] Meixing Xu,‡[b] Alexios Grigoropoulos, §[a] Ioannis Bratsos,[c] Catherine P. Raptopoulou,[c] Vassilis Psycharis,[c] Shang-Da Jiang *[b,d] and Panayotis Kyritsis *[a]

The synthesis and the structural characterization of the octahedral *trans*-[Co{(OPPh$_2$)(EPPh$_2$)N}$_2$(dmf)$_2$], E = S (**1**), Se (**2**), complexes is described. These complexes are formed by crystallization of the corresponding tetrahedral [Co{(OPPh$_2$)(EPPh$_2$)N}$_2$] complexes in the presence of dimethylformamide (dmf) and are the first examples of intact octahedral Co(II) complexes bearing dichalcogenidoimidodiphosphinato ligands. X-ray crystallography studies revealed a *trans*-CoO$_4$E$_2$ first coordination sphere consisting of two chelating (OPPh$_2$)(EPPh$_2$)N$^-$ ligands, as well as two dmf molecules coordinated *via* their O atoms. The isomorphous complexes **1** and **2** were studied by Direct Current magnetometry and shown to exhibit axial magnetic anisotropy. This finding was unequivocally confirmed by magnetic susceptibility measurements on an oriented crystal of complex **1**, which clearly defined its easy axis of magnetization. Alternating Current magnetometry studies revealed field-induced slow relaxation of magnetization for both complexes, the characteristics of which are compared with those of other octahedral Co(II) complexes. The effects of the Se- *vs.* S-coordination on the magnetic anisotropy and relaxation properties of these and other 3d metal complexes are discussed.

Received 1st February 2019,
Accepted 4th April 2019

DOI: 10.1039/c9qi00135b

rsc.li/frontiers-inorganic

Introduction

Ever since their discovery in the early 1990s,[1,2] single-molecule magnets (SMMs) have attracted great interest,[3] due to their potential applications in high-density data storage, molecular spintronics and quantum computation devices,[4] as well as their interesting magnetothermal properties.[5] These compounds exhibit slow relaxation of their magnetization and magnetic hysteresis below the corresponding blocking temperature, of pure molecular origin. The multinuclear [Mn$_{12}$O$_{12}$(CH$_3$CO$_2$)$_{16}$(H$_2$O)$_4$] complex is the first molecular compound shown to exhibit an activation barrier (U_{eff}) for the relaxation of its magnetization.[1,2,6] Following this observation, numerous multinuclear complexes, involving 3d metal ions, have been explored.[7,8] The magnitude of U_{eff} in a SMM is controlled by the total spin, S, of the ground state, and the magnetic anisotropy of the system, expressed *via* the axial D zero-field splitting (zfs) component. Specifically, U_{eff} is tentatively considered to be equal to $S^2|D|$ or $(S^2 - 1/4)|D|$ for integer and non-integer spin systems, respectively. Therefore, the desired characteristics of SMMs are a large ground spin state S and a large magnetic anisotropy, D. Large S can be achieved *via* predominant ferromagnetic interactions in multinuclear metal complexes,[9,10] but, due to their overall high symmetry, such systems exhibit remarkably small magnetic anisotropies (*i.e.* usually $D < 1$ cm^{-1}).[11] On the other hand, the principles of synthetic coordination chemistry, concerning the interplay between the metal ion and the ligands employed, can be

[a]*Inorganic Chemistry Laboratory, Department of Chemistry, National and Kapodistrian University of Athens, Panepistimiopolis, GR-15771 Athens, Greece. E-mail: kyritsis@chem.uoa.gr*
[b]*College of Chemistry and Molecular Engineering, Beijing National Laboratory for Molecular Sciences, Beijing Key Laboratory of Magnetoelectric Materials and Devices, Peking University, Beijing 100871, P. R. China. E-mail: jiangsd@pku.edu.cn*
[c]*NCSR "Demokritos", Institute of Nanoscience and Nanotechnology, 15310 Aghia Paraskevi, Athens, Greece*
[d]*Beijing Academy of Quantum Information Sciences, West Bld.#3, No. 10 Xibeiwang East Rd., Haidian District, Beijing 100193, P. R. China*

†Electronic supplementary information (ESI) available: Complexes **1** and **2**: crystal data and crystallographic information files, orientation of a crystal of **1**, IR spectroscopy, PXRD and magnetometry data for **1** and **2**, literature survey on slowly-relaxing octahedral Co(II) complexes. CCDC 1892040 and 1892041. For ESI and crystallographic data in CIF or other electronic format see DOI: 10.1039/c9qi00135b

‡These authors contributed equally.

§Present address: Department of Chemistry, Materials Innovation Factory, University of Liverpool, Liverpool L7 3NY, U.K.

applied much more effectively on mononuclear complexes, potentially leading to coordination spheres of the desired structural and, hence, magnetic properties.[12] For that reason, research efforts have been recently directed towards the synthesis of mononuclear complexes of lanthanides[13,14] and actinides,[15] which exhibit remarkably large magnetic anisotropies, owing to large and unquenched spin–orbit coupling (SOC). Moreover, in some complexes of this type, blocking temperatures approaching that of liquid nitrogen (77 K) have been achieved[16–18] thus opening up the prospects of potential technological applications.

In an effort to master a synthetic control over the magnitude of D, a large number of 3d-based mononuclear complexes have been under extensive experimental[19–22] or computational[23,24] investigation. A trigonal pyramidal high spin Fe(II) complex is the first 3d metal-based mononuclear complex shown to exhibit field-induced slow relaxation of its magnetization.[25] Following that report, slow relaxation of magnetization has been established for complexes of Cr(II), Mn(III), Mn(IV), Fe(I), Fe(II), Fe(III), Co(I), Co(II), Ni(I), Ni(II), Cu(II), Cu(III), Re(IV),[19–22] and more recently of V(IV),[26,27] Mn(II)[28,29] and Ru(III).[30]

Complexes of Co(II) constitute the largest family of 3d-metal-based complexes showing slow relaxation of their magnetization.[22,31] It should be stressed that the tetrahedral S = 3/2 $(PPh_4)_2[Co(SPh)_4]$ complex[32,33] bearing a $Co(II)S_4$ core, was the first mononuclear 3d metal complex to exhibit slow relaxation of its magnetization in the absence of a Direct Current (DC) magnetic field.[34–37] Along these lines, tetrahedral $[Co\{(EP^iPr_2)_2N\}_2]$, E = S,[38] Se,[38] Te,[39] complexes, bearing dichalcogenidoimidodiphosphinato ligands[40] and $Co(II)E_4$ cores, exhibit slow relaxation of their magnetization, which was also observed in the absence of DC magnetic field for the E = Se, Te, complexes. On the other hand, high-spin, S = 3/2, octahedral Co(II) complexes exhibit magnetic anisotropy that can be tuned through appropriate structural modifications, for instance axial elongation or compression of an octahedral coordination sphere, leading to axial anisotropy (very small Δ_{rh}) and the presence of either easy axis ($\Delta_{ax} < 0$) or easy plane ($\Delta_{ax} > 0$), of magnetization, respectively (Δ_{ax} is the axial and Δ_{rh} the rhombic crystal field parameter, *vide infra*).[41] Ever since the $[Co(dmphen)_2(NCS)_2]$ complex (dmphen = 2,9-dimethyl-1,10-phenanthroline) has been shown to exhibit field-induced slow relaxation of its magnetization,[42] the relaxation properties of a large number of octahedral high-spin Co(II) complexes, exhibiting coordination spheres dominated Co–N or Co–O bonds, have been investigated (Table S1†).

Some of us have reported the conversion of the tetrahedral complexes $[Ni\{(OPPh_2)(EPPh_2)N\}_2]$, E = S,[43] Se,[44] to octahedral *trans*-$[Ni\{(OPPh_2)(EPPh_2)N\}_2(sol)_2]$, sol = dmf,[44] thf,[45] dmso.[46] Accurate zfs parameters for the latter S = 1 complexes were determined by high-frequency and -field EPR spectroscopy (HFEPR).[45,46] In the work presented herein, the analogous conversion of tetrahedral $[Co\{(OPPh_2)(EPPh_2)N\}_2]$ E = S,[47] Se,[44] to octahedral *trans*-$[Co\{(OPPh_2)(EPPh_2)N\}_2(dmf)_2]$ E = S (**1**), Se (**2**), is reported. Studies on the S = 3/2 complexes **1** and **2** by DC and Alternating Current (AC) magnetometry reveals that they exhibit field-induced slow relaxation of magnetization. The observed effects of the nature of the donor atoms E = S or Se, on the magnetic behavior of complexes **1** and **2**, are discussed, and comparisons with other octahedral Co(II) complexes exhibiting field-induced slow relaxation of magnetization are made.

Results and discussion

Synthesis and IR spectroscopic characterization

Complexes **1** and **2** were obtained as crystalline products, upon slow diffusion of the coordinating solvent dmf into dichloromethane solutions of tetrahedral $[Co\{(OPPh_2)(EPPh_2)N\}_2]$, E = S,[47] Se.[44] The same procedure has been previously employed for the preparation of the analogous Ni(II) octahedral complexes *trans*-$[Ni\{(OPPh_2)(EPPh_2)N\}_2(dmf)_2]$.[44] The most characteristic IR bands of complexes **1** and **2** (Fig. S1 and S2,† respectively), as well as their comparison with those of the corresponding ligands, are shown and analyzed in the ESI.†

X-ray crystallography

Single crystal X-ray diffraction revealed that complexes **1** and **2** are isomorphous (crystallographic data for both compounds are listed in Table S2†). A detailed crystallographic description is presented for complex **1** and, in parallel, the basic characteristics of complex **2** are also discussed. The molecular structure of **1** is shown in Fig. 1a and that of **2** in Fig. S3.† The isomorphous relationship between **1** and **2** is further supported by the overlay plot presented in Fig. 1b. Bond distance and bond angle values of **1** and **2** are listed in Table 1. Both compounds crystallize in the $P\bar{1}$ space group and possess a center of symmetry, occupied by a Co(II) ion. The latter is coordinated to two $(OPPh_2)(EPPh_2)N^-$ ligands and two dmf molecules, both being centrosymmetrically (*trans*) related, resulting in the stoichiometric formula *trans*-$[Co\{(OPPh_2)(EPPh_2)N\}_2(dmf)_2]$, E = S, Se. To the best of our knowledge, this is the first report of intact octahedral Co(II) complexes bearing dichalcogenidoimidodiphosphinato ligands. The previously reported octahedral $[Co\{(OP^iPr_2)(OP^iPr_2)NH\text{-}\kappa^2O,O'\}_3]^{2+}$ species has been identified in crystals also comprising tetrahedral $[Co\{(OP^iPr_2)(OP^iPr_2)NH\text{-}\kappa^2O,O'\}_2Cl_2]$ and $[CoCl_4]^{2-}$ species.[48]

The crystal structure of both **1** and **2** consists of discrete monomeric molecules, exhibiting distorted octahedral *trans*-CoO_4E_2 cores. In the following, the Co–O bond involving the chelating ligand will be referred to as $Co–O_L$, in order to distinguish it from the Co–O41 bond involving coordination of dmf. The equatorial sites of the octahedron are occupied by four oxygen atoms with $Co–O_L$ and Co–O41 bond lengths in the range 2.022(2)–2.105(2) Å. The respective $Co–O_L$ and Co–O41 bond lengths (Fig. 1) of complexes **1** and **2** are almost equal (Table 1). The two axial sites are occupied by centrosymmetrically related S or Se atoms of the chelating ligand, with Co–E bond lengths of 2.5853(8) for **1** (E = S) and 2.6892(3) Å for **2** (E = Se), resulting in an axially elongated octahedral

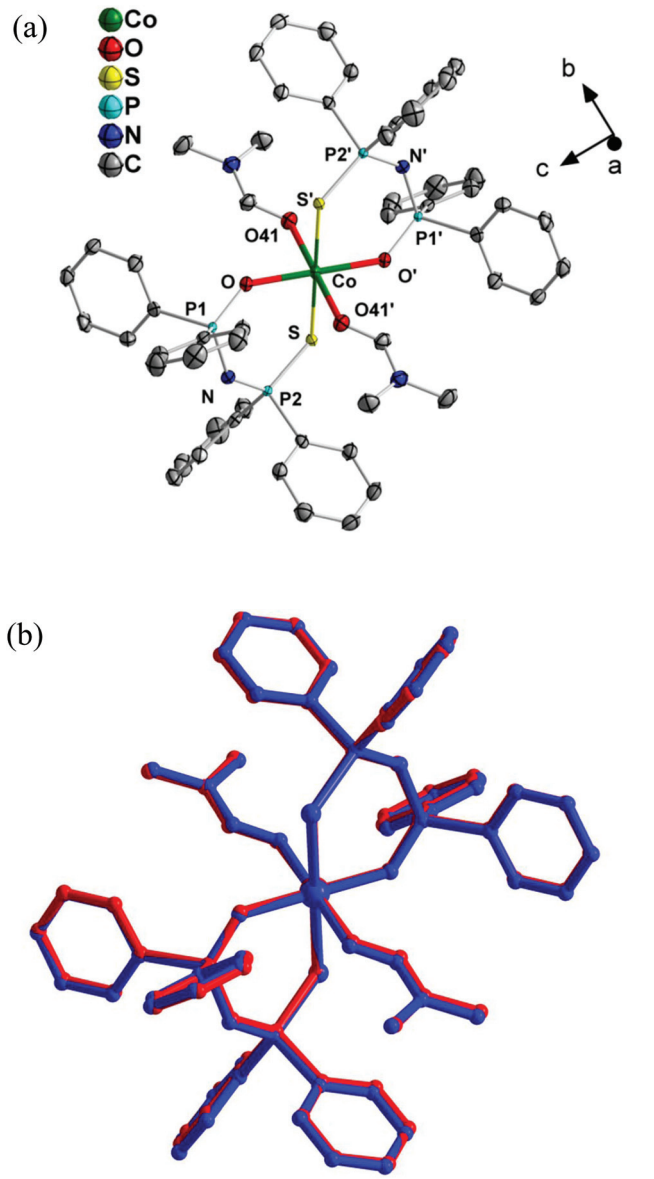

Fig. 1 (a) Ortep plot of complex **1**. Thermal ellipsoids are presented at a 50% probability level. (b) Overlay plot of the molecular structures of complexes **1** (red) and **2** (blue). Symmetry code: (′): $-x, -y, -z$.

coordination sphere (Fig. 1 and S3†). A similar axial elongation was observed in octahedral *trans*-[Ni{$(OPPh_2)(EPPh_2)N\}_2$(dmf)$_2$][44] and *trans*-[Co{$(OP(O^iPr)_2(SCPh)N$-$\kappa^2O,S\}_2${$OP(O^iPr)_2(SCPh)NH$-$\kappa^1O\}_2$].[49]

The Co–O_L bond lengths of complex **1** are larger by only 0.04 Å compared to those of tetrahedral [Co{$(OPPh_2)(SPPh_2)N\}_2$] (average 1.980 Å).[47] By contrast, the Co–S bonds are significantly elongated by 0.25 Å and 0.27 Å/0.26 Å, compared to [Co{$(OPPh_2)(SPPh_2)N\}_2$] (average 2.331 Å)[47] and tetrahedral [Co{$(SPPh_2)_2N\}_2$] (average, in two reported structures: 2.316 Å (ref. 50*a*) and 2.324 Å (ref. 51)), respectively. For complex **2**, the Co–O_L bond lengths are larger by 0.06 Å compared to those of tetrahedral [Co{$(OPPh_2)(SePPh_2)N\}_2$] (average 1.961 Å).[44] However, the Co–Se bond lengths are larger by 0.24 Å and 0.26/0.27 Å, respectively, compared to those of [Co{$(OPPh_2)(SePPh_2)N\}_2$] (average 2.444 Å)[44] and tetrahedral [Co{$(SePPh_2)_2N\}_2$] (average 2.4323 [50a] and 2.415 Å (ref. 50*b*)). The above comparisons reveal a remarkable weakening of the Co–E bonds in complexes **1** and **2**, compared to those of [Co{$(EPPh_2)_2N\}_2$], E = S,[50a,51] Se.[50] The P–N–P angles of **1** and **2** (133.0° and 133.2°, respectively) are increased slightly compared to those of the $(OPPh)_2(SPPh_2)NH$[52] and {$OP(OPh)_2$}$(SePPh_2)NH$[53] ligands (132.9° and 131.8°, respectively). The differences between the respective P–O, P–N and P–E, E = S, Se, bond lengths of these ligands and complexes **1** and **2** (not shown) are consistent with delocalization of π-electronic density over the Co–O–P–N–P–E, E = S, Se, chelate rings, upon their deprotonation and coordination to Co(II).[54,55]

Table 1 Selected bond lengths (Å) and angles (°) of complexes **1** and **2**

1		**2**	
Bond lengths (Å)			
Co–O	2.022(2)	Co–O	2.025(2)
Co–O41	2.104(2)	Co–O41	2.105(2)
Co–S	2.5853(8)	Co–Se	2.6892(3)
Bond angles (°)			
O–Co–S	93.24(6)	O–Co–Se	93.05(5)
O–Co–S′	86.76(6)	O–Co–Se′	86.95(5)
O41–Co–S	90.90(6)	O41–Co–Se	89.94(5)
O41–Co–S′	89.10(6)	O41–Co–Se′	90.06(5)
O–Co–O41	89.50(8)	O–Co–O41	89.58(7)
O–Co–O41′	90.50(8)	O–Co–O41′	90.42(7)
O41–Co–O41′	180.0	O41–Co–O41′	180.0
O–Co–O′	180.0	O–Co–O′	180.0
S–Co–S′	180.0	Se–Co–Se′	180.0

Symmetry code: (′): $-x, -y, -z$.

The distortion from the ideal octahedral geometry of complexes **1** and **2** is further verified by the different endocyclic (93.24° and 93.05°, respectively) and exocyclic (86.76° and 86.95°, respectively), equatorial O–Co–E angles. Similar structural features were observed in the analogous *trans*-[Ni{$(OPPh_2)(EPPh_2)N\}_2$(dmf)$_2$] complexes, E = S, Se, exhibiting equatorial endocyclic (93.88° and 93.27°) and exocyclic (86.12° and 86.73°) angles, respectively.[44] In both **1** and **2**, the two non-planar equatorial six-membered Co–O–P–N–P–E, E = S, Se, chelating rings exhibit pseudo-boat conformations, with the Co and N atoms being the "bow" and the "stern" of the boat.

DC magnetometry studies

Complexes **1** and **2** remain intact after magnetometry measurements, as deduced by elemental analysis (*vide infra*). Moreover, the experimental powder X-ray diffraction (PXRD) pattern of complex **1** is in good agreement with the corresponding theoretical one (Fig. S4†). For complex **2**, although a good match is observed for peaks at $2\theta < 10°$ (Fig. S5†), above this angle deviations are observed, probably caused by the coarse-grained crystalline nature of the sample, as we have not ground extensively both samples, in order to avoid their eventual damage.

It should also be stressed that in analyzing magnetometric data, the employment of a spin Hamiltonian comprising

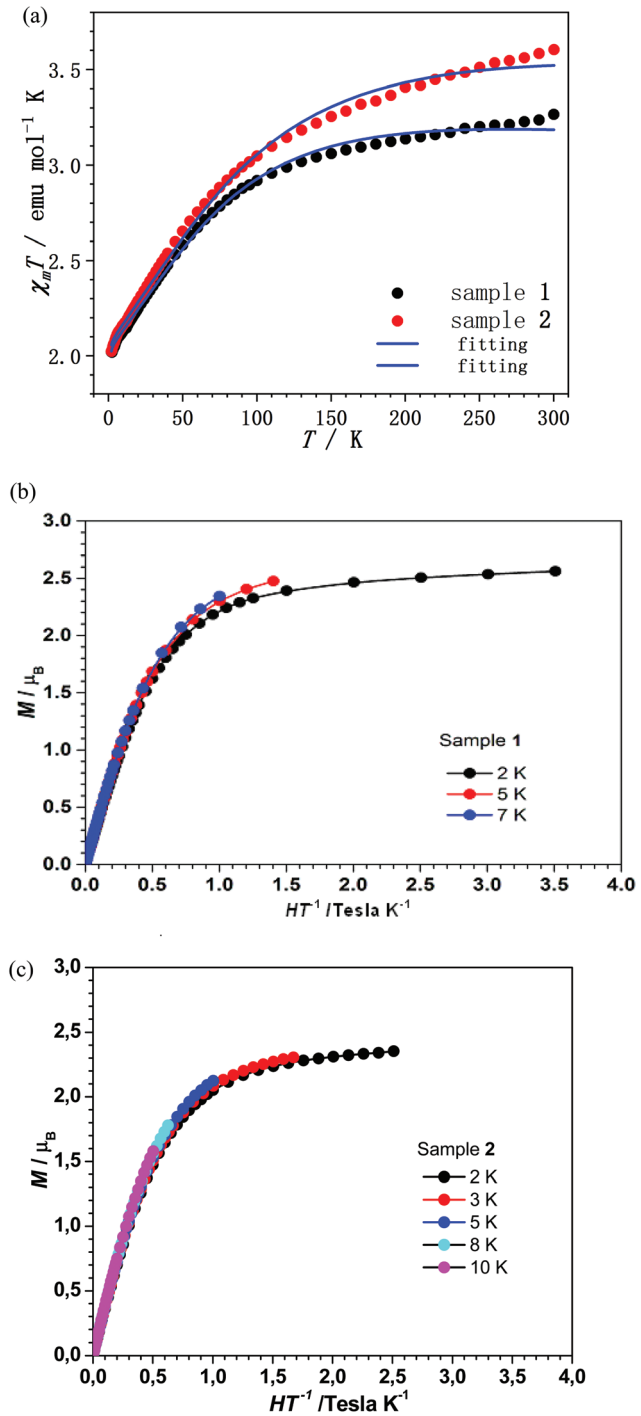

Fig. 2 (a) Temperature-dependent $\chi_m T$ data for **1** and **2** between 2 and 300 K under a DC field of 1000 Oe. (b, c) *M vs. H*/*T* plots for **1** and **2**, respectively, at low temperature values.

Table 2 Griffith Hamiltonian parameters and U_{eff} values of complexes **1** and **2**

Complex	g_z	Δ_{ax} (cm^{-1})	Δ_{rh} (cm^{-1})	λ (cm^{-1})	U_{eff} (cm^{-1})
1	2.40	−487.4	0.15	−138.6	23.6
2	2.78	−448.4	−0.43	−153.3	18.1

Zeeman (g) and zero-field splitting terms D and E is appropriate only for orbit momentum quenched systems. In systems exhibiting either T_{2g} or E_g ground electronic states, such a spin Hamiltonian cannot be applied.[41,56,57] Unfortunately, the latter has been frequently employed for octahedral Co(II) complexes, affording the D and E data listed in Table S1,† but, owing to the above discrepancy, these data should be treated very cautiously.

The temperature-dependent magnetic susceptibility of complexes **1** and **2** was measured under a DC field of 1000 Oe, in the temperature range between 2 and 300 K (Fig. 2a). The $\chi_m T$ value at 300 K is 3.27 emu mol^{-1} K for **1** and 3.60 emu mol^{-1} K for **2**, which are much larger than the theoretical value of 1.875 emu mol^{-1} K for a spin-only high spin Co(II) system.[58] It is worth noting the strong temperature dependence of $\chi_m T$ which is different from the typical spin-only magnetic anisotropy behaviour. These data suggest the existence of significant SOC of the spin carriers.

The low-temperature magnetization of **1** and **2** was measured at different DC fields below 4 T. The nearly superposition of the *M vs. H*/*T* plots (Fig. 2b and c) implies that the magnetic field is too small to vary the population of the electronic fine structures at low temperature. This is strong evidence for the existence of significant magnetic anisotropy in complexes **1** and **2**. However, owing to the significant contribution of the orbital angular momentum in octahedral complexes **1** and **2**, the ANISOFIT 2.0 software[59] is not suitable to fit the data. To describe the DC magnetic properties of these systems, the Griffith Hamiltonian (1) was employed, which includes the Δ_{ax} and Δ_{rh} crystal field parameters (*vide supra*) and explicitly takes into account the unquenched orbital angular momentum of the Co(II) ion:[60–62]

$$\hat{H} = -\frac{3}{2}\kappa\lambda\hat{L}\hat{S} + \Delta_{ax}\left[\hat{L}_Z{}^2 - \frac{1}{3}L(L+1)\right] + \Delta_{rh}(\hat{L}_X{}^2 - \hat{L}_Y{}^2) + \mu_B H\left(g_e\hat{S} - \frac{3}{2}\kappa L\right) \quad (1)$$

In eqn (1), λ is the spin–orbit coupling parameter and κ is the reduction factor of the orbital angular momentum. The fitting results were obtained through the use of the PHI software.[63] By setting $\kappa = -1.3$ and fixing $g_x = g_y = 2$ (implying axial magnetic anisotropy, *vide infra*), the parameters listed in Table 2 were obtained. Both complexes **1** and **2** exhibit very small Δ_{rh} values and, therefore, an axial type of magnetic anisotropy. Moreover, the fact that in both systems $\Delta_{ax} < 0$ reveals the existence of an easy axis of magnetization.

Angular-dependent magnetometry studies of complex 1

A suitably large crystal of complex **1** was oriented as shown in Fig. S6† and studied by magnetometry. Strong anisotropy of the magnetization was observed for the rotations along experimentally defined *X*- (Fig. 3a) and *Z*- (Fig. 3c) directions, whereas along the *Y*-direction (Fig. 3b) the magnetic susceptibility was found to be more isotropic and having a smaller overall value. This observation provides strong evidence of axial anisotropy and the presence of an easy axis of magnetiza-

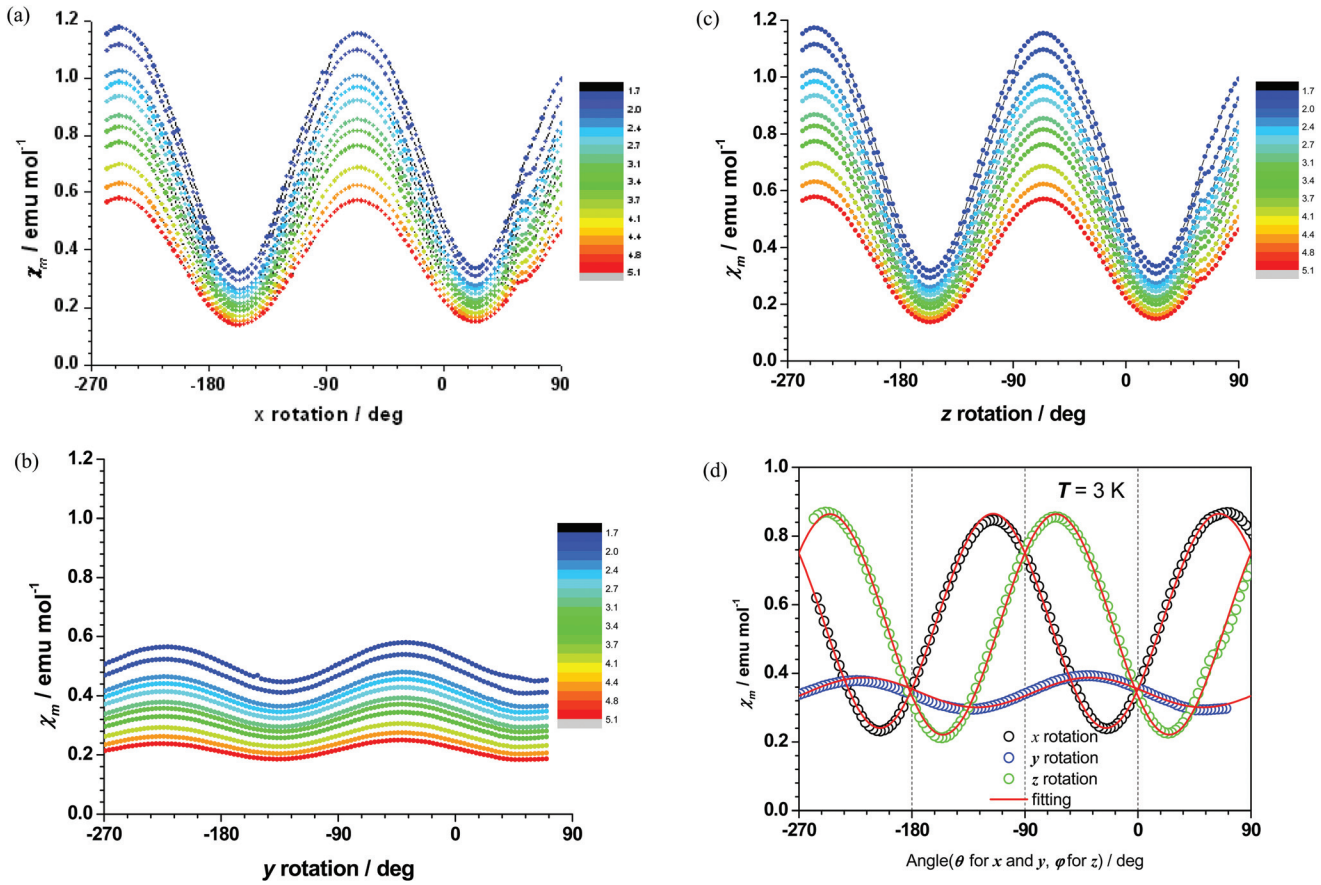

Fig. 3 (a, b, c, respectively) The magnetic susceptibility of complex **1** along the *X, Y, Z* directions between 1.8 K and 5 K. (d) Angular dependence of the magnetic susceptibility of **1** at 3 K under a DC field of 1000 Oe (circle). The red solid lines represent the best fitting based on the experimental data.

tion, confirming the data obtained by DC magnetometry (*vide supra*). The susceptibility tensor with respect to the experimental frame is determined by simultaneously fitting the three rotation sine curves at 3 K, as depicted in Fig. 3d. The principle axes and the corresponding susceptibility values are therefore the eigenvectors and eigenvalues of the tensor. As shown in Fig. 4a, the $\chi_{\mathrm{m}}T$ value along the easy axis is larger than those along the other two axes, thus unequivocally confirming that complex **1** exhibits axial anisotropy and possesses an easy axis of magnetization. The orientation of the experimentally determined magnetization principal axes, with respect to the *XYZ* frame (Fig. S6†), is shown in Fig. 4b. Attempts were made to carry out a similar study on a crystal of complex **2**, but its smaller size, compared to that of complex **1**, precluded such experiments.

AC magnetometry studies

To probe the dynamic magnetic behavior of complexes **1** and **2**, their AC magnetic susceptibility was measured at various frequencies and temperatures. Under zero-applied DC magnetic field, no slow relaxation of magnetization was observed in the 10–1000 Hz and 100–10 000 Hz range for **1** and **2**, respectively (Fig. S7a and d†). These observations provide evidence of a fast quantum tunneling of magnetization (QTM), which is stemming from extensive mixing of excited states into the ground states.[64,65] On the other hand, both complexes **1** and **2** exhibit slow magnetic relaxations under an external DC field (300 and 2000 Oe, respectively), which can prominently suppress the QTM process (Fig. S7b, c and e†). It should be noted that, to the best of our knowledge, all complexes listed in Table S1† exhibit slow relaxation of magnetization only in the presence of an external DC magnetic field.

The relaxation times τ of complexes **1** and **2** were extracted by fitting χ' and χ'' to a generalized Debye model. The corresponding Cole–Cole plots for complexes **1** and **2** are shown in Fig. S8 and S9,† respectively. The distribution of the corresponding α values is very narrow, indicating a single relaxation process. By fitting $\ln\tau$ *vs.* T^{-1} on the basis of an Arrhenius expression (Fig. 5c and 6b), effective energy barriers U_{eff} = 23.6 cm^{-1} for **1** (under 300 Oe) and U_{eff} = 18.1 cm^{-1} for **2** (under 2000 Oe) were obtained. For complex **2**, due to the curvature of the plot, in addition to the Arrhenius-type fit performed at the high temperature region, a fit according to the equation $\tau^{-1} = CT^{n}$ for a Raman relaxation process was carried out (Fig. 6b). We note that the U_{eff} values of complexes **1** and **2** are significantly smaller compared to the corresponding Δ_{ax}

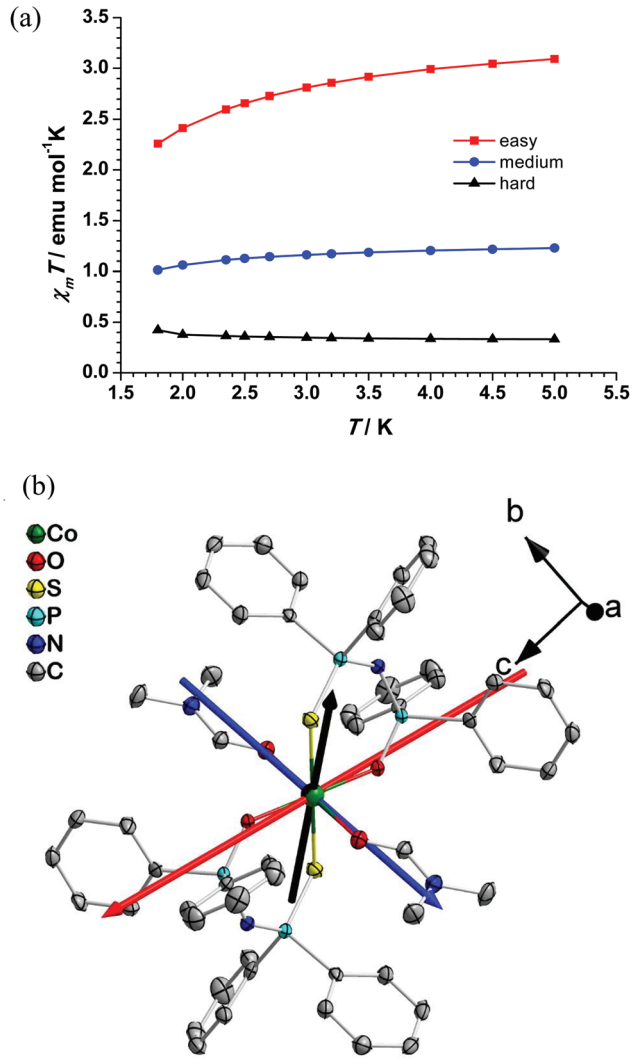

Fig. 4 (a) The $\chi_m T$ values of complex **1** determined by angular-dependent magnetometry measurements along the easy (red), medium (blue) and hard (black) axes. (b) Experimentally determined magnetization principal axes, with the red arrow being the easy axis.

parameters of the two complexes (Table 2) and fall between the extremes of values corresponding to the Co(II) octahedral complexes listed in Table S1.†

Effects of S/Se metal-coordination

This work reports on the magnetic anisotropy and relaxation properties of octahedral complexes bearing Co–E, E = S, Se, bonds. The Δ_{ax} and Δ_{rh} values of complexes **1** and **2** reveal that replacing S in **1** by Se in **2** leads to smaller axial and larger rhombic anisotropy (Table 2). The smaller magnitude of Δ_{ax} in complex **2** may be caused by the greater degree of covalency of the Co–Se bond compared to that of the Co–S bond, leading to stronger quenching of the metal ion's SOC, due to the ligand field, in complex **2**.[22] On the other hand, the magnetic anisotropy is also expected to be affected by the nature of the ligands. For instance, in some systems, heavier donor atoms have been shown to confer stronger axial anisotropy, most likely due to their stronger SOC (*vide infra*). However, the respective operating effects cannot be quantified in a straightforward manner, because the local coordination geometry of the metal ions, as well as the metal–ligand covalency, may vary among different systems.

A similar trend, to that established for complexes **1** and **2**, has been previously observed concerning *trans*-[Ni{$(OPPh_2)(EPPh_2)N$}$_2$(sol)$_2$], E = S, Se, for sol = dmf, thf, in which the E = Se complex exhibits smaller D but larger E/D.[45] On the other hand, both smaller D and E/D were observed for the Se-containing complex when sol = dmso, as determined by HFEPR.[46] It should be also noted that the tetrahedral S = 3/2 [Co{$(EP^iPr_2)(E^iPr_2)N$}$_2$] complexes, exhibit similar experimentally determined axial anisotropies ($D \sim -30.5$, E = S and -30.4 cm^{-1} E = Se),[38] whereas the E = Te analogue shows larger axial anisotropy (D = -45.1 cm^{-1}).[39] No significant differences have been observed in the magnetic anisotropy between tetrahedral [Co{$(EPPh_2)_2N$}$_2$], E = S (-11.9 cm^{-1}),[66] Se (-15.8 cm^{-1}).[39] On the other hand, a trend of progressively larger axial anisotropies was established for tetrahedral $[Co(EPh)_4]^{2-}$ complexes along the E = O, S, Se, series.[67] Furthermore, in the case of the tetrahedral S = 2 complexes [Fe{$(EPPh_2)_2N$}$_2$], the E = Se complex[68] exhibits similar axial but slightly larger rhombic anisotropy, compared with that of the E = S one,[69] as determined by HFEPR. Unlike the moderate effects, on the magnetic anisotropy, of Se- *versus* S-coordination to the above 3d metal ions, the presence of heavier p-block elements like Se enhances the magnetic anisotropy of $S = \frac{1}{2}$ radicals, due to increased SOC effects.[70,71]

In the above context, the coordination of heavier halogeno ligands to Ni(II)[72] or Cr(II)[73] has been shown to confer increased axial anisotropies. Similar effects, on the magnitude of the axial anisotropy due to the coordination of heavier halides, have also been established in tetrahedral[74–80] Co(II) complexes, in some instances imposing a concomitant change in the sign of D as well.[76,77] On the other hand, contrary to the above observations, lower axial anisotropy due to the coordination of heavier halides has been observed in square-pyramidal[81,82] and pentagonal bipyramidal[83] Co(II) complexes.

With respect to the dynamic magnetic properties, complex **2**, bearing a CoO_4Se_2 coordination sphere, exhibits smaller U_{eff} energy barrier (18.1 cm^{-1}) than that of complex **1** (23.6 cm^{-1}) bearing a CoO_4S_2 one (Tables 2 and S1†). This observation is compatible with the fact that complex **2** exhibits smaller axial and larger rhombic anisotropy compared with that of complex **1** (*vide supra*). In the same context, the U_{eff} values and relaxation mechanisms for the series of tetrahedral S = 3/2 [Co{$(EP^iPr_2)_2N$}$_2$] complexes, E = S (54 cm^{-1}, at 0.2 Tesla, Orbach mechanism),[38] Se (Raman mechanism, at zero-field),[38] Te (22 cm^{-1}, Orbach mechanism, at zero-field),[39] reveal profound effects of the nature of the donor atom E. On the other hand, the U_{eff} values for the series of tetrahedral $[Co(EPh)_4]^{2-}$ complexes, E = O (21 cm^{-1}), S (21 cm^{-1}), Se (19 cm^{-1}), are effectively the same.[67]

Owing to the above observations that do not establish clear trends, additional experimental and computation work is

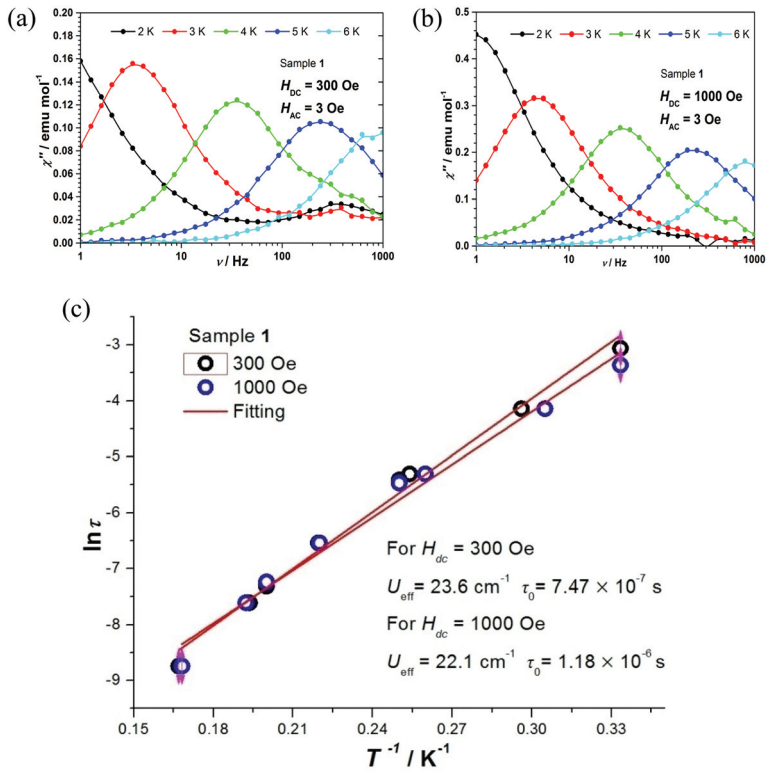

Fig. 5 Complex **1**: Frequency dependence of the out-of-phase AC susceptibility under 300 Oe (a) and 1000 Oe (b) from 2 K to 6 K. (c) $\ln\tau$ *vs.* T^{-1} under 300 Oe (black circles) and 1000 Oe (blue circles). Red lines represent Arrhenius fit plots.

needed in order to fully elucidate the effects, on either magnetic anisotropy or relaxation properties, of metal–ligand coordination *via* heavier donor atoms.

Conclusions

The synthesis and characterization of *trans*-[Co{$(OPPh_2)(EPPh_2)N$}$_2$$(dmf)_2$], E = S, Se, complexes is described, based on the crystallization of tetrahedral [Co{$(OPPh_2)(EPPh_2)N$}$_2$] in the presence of dmf. X-ray crystallography studies revealed that complexes **1** and **2** are isomorphous and they exhibit axially elongated octahedral *trans*-CoO_4E_2, E = S, Se, coordination spheres. DC magnetometry analysis established that both complexes exhibit axial magnetic anisotropy, which, for complex **1**, was unequivocally confirmed by magnetometry studies on an oriented crystal of this complex, also revealing an easy axis of magnetization.

This work extends the dataset of octahedral Co(II) complexes exhibiting field-induced slow relaxation of magnetization, which are dominated by the presence of Co–O or Co–N bonds in their coordination spheres (Table S1†). Moreover, AC magnetometry studies probed the dynamic magnetic properties of the two complexes, revealing an apparently smaller U_{eff} value for the Se-containing complex **2** compared with that of the S-containing complex **1** (Tables 2 and S1†). Complexes **1** and **2** extend the set of 3d-based complexes bearing dichalcogenidoimidodiphosphinato ligands[40] and exhibiting slow relaxation of magnetization, so far consisting of tetrahedral Co(II)[38,39] and octahedral Mn(III) complexes.[84]

Materials and methods

General

The ligands $(OPPh_2)(EPPh_2)NH$, E = S,[52] Se,[52] and complexes [Co{$(OPPh_2)(EPPh_2)N$}$_2$] E = S,[47] Se,[44] were prepared according to published procedures. Elemental analyses were performed prior and after magnetometry measurements using Elementar Vario MICRO CUBE (Germany). IR spectra were run in the range 4000–200 cm^{-1} on a PerkinElmer 883 IR spectrophotometer, as KBr pellets. The PXRD patterns were recorded on a Rigaku R-AXIS IV Imaging Plate Detector mounted on a Rigaku RU-H3R Rotating Copper Anode X-ray Generator (λ = 1.54 Å). The samples were slightly ground, inserted in capillary mark tubes (ID = 1 mm) and attached to a rotating stage. The capillaries were spinned (36° min^{-1}) during the measurement.

Chemical synthesis

***trans*-[Co{$(OPPh_2)(SPPh_2)N$}$_2$$(dmf)_2$] (1).** During the crystallization process by slow diffusion of dmf into dichloromethane solutions of tetrahedral [Co{$(OPPh_2)(SPPh_2)N$}$_2$] at room temperature, the color gradually changed from blue to purple. Acicular purple crystals were grown after about one week,

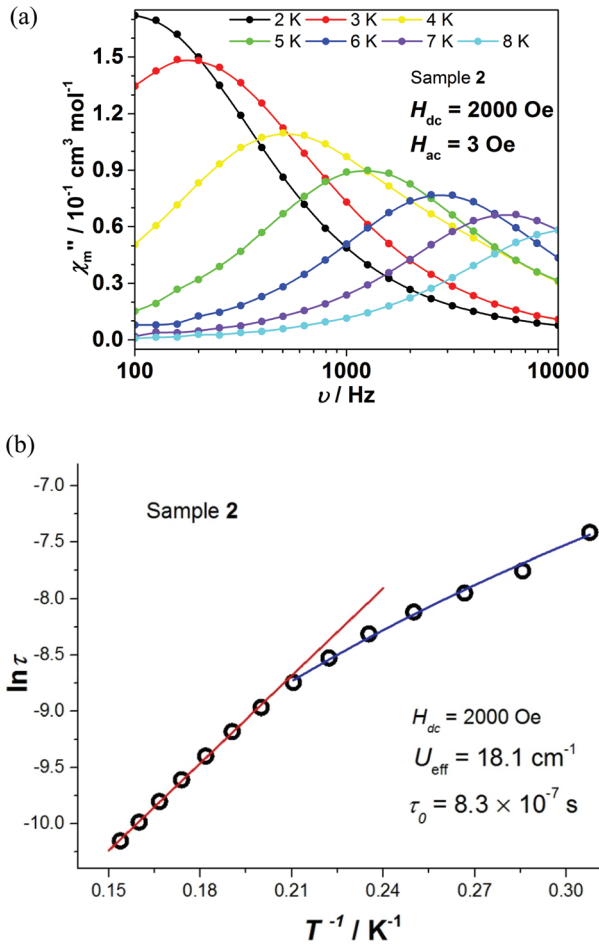

Fig. 6 Complex **2**: (a) Frequency dependence of the out-of-phase AC susceptibility under 2000 Oe from 2 K to 8 K. (b) Arrhenius-type ln τ *vs.* T^{-1} fit (high temperature region, red line) and Raman relaxation fit $\tau^{-1} = CT^n$ (low temperature region, blue line, with fitting parameters C = 30.4 and n = 3.4), under 2000 Oe.

which were shown by X-ray crystallography to correspond to *trans*-[Co{(OPPh$_2$)(SPPh$_2$)N}$_2$(dmf)$_2$]. IR (cm^{-1}) ν(CO) 1644, ν_{as}(P$_2$N) 1232, ν(PO) 1125, 1086, ν(PS) 593. Calcd (%), $C_{54}H_{54}O_4N_4P_4S_2Co_1$: C, 60.62; H, 5.09; N, 5.24. Found, prior the magnetometry measurements: C, 60.55; H, 5.08; N, 5.24; found, after the magnetometry measurements: C, 60.44; H, 5.05; N, 5.24.

***trans*-[Co{(OPPh$_2$)(SePPh$_2$)N}$_2$(dmf)$_2$] (2).** The above crystallization procedure was also applied for tetrahedral [Co{(OPPh$_2$)(SePPh$_2$)N}$_2$]. Cubic purple crystals were grown after one week, which were shown by X-ray crystallography to correspond to *trans*-[Co{(OPPh$_2$)(SePPh$_2$)N}$_2$(dmf)$_2$]. IR (cm^{-1}) ν(CO) 1648, ν_{as}(P$_2$N) 1233, ν(PO) 1129, 1089, ν(PSe) 560, 542. Calcd (%), $C_{54}H_{54}O_4N_4P_4Se_2Co_1$: C, 55.73; H, 4.68; N, 4.81. Found, before the magnetometry measurements: C, 55.68; H, 4.69; N, 4.82; found, after the magnetometry measurements: C, 55.77; H, 4.55; N, 4.78.

X-ray crystallography. Crystals of complexes **1** (0.07 × 0.13 × 0.46 mm) and **2** (0.29 × 0.30 × 0.30 mm) were taken from the mother liquor and immediately cooled to 160 K. Diffraction measurements were made on a Rigaku R-AXIS SPIDER Image Plate diffractometer using graphite monochromated Cu Kα radiation. Data collection (ω-scans) and processing (cell refinement, data reduction and empirical absorption correction) were performed using the CrystalClear program package.[85] The structures were solved by direct methods using SHELXS ver.2013/1 and refined by full-matrix least-squares techniques on F^2 with SHELXL ver.2014/6.[86] Hydrogen atoms were located by difference maps and were refined isotropically or were introduced at calculated positions as riding on bonded atoms. All non-hydrogen atoms were refined anisotropically. Plots of the structures were drawn using the Diamond 3 program package.[87]

Magnetometry. DC and AC magnetic susceptibility measurements (in 10–1000 Hz) for complex **1** were performed on a Quantum Design MPMSXL7 SQUID system. The powder sample was wrapped in parafilm and fixed in a gel capsule. The diamagnetic correction of the measured susceptibility was calculated *via* Pascal's constants, as well as the diamagnetism from the parafilm and the capsule.

DC magnetic susceptibility measurements for complex **2** were performed on a Quantum Design MPMSXL5 SQUID system. AC susceptibility for **2** was measured on a Quantum Design PPMS-9 with ACMS accessories in the 100–10 000 Hz.

Angular-dependent magnetometric studies on a single crystal of complex **1** were carried out on the MPMSXL7 SQUID magnetometer equipped with a horizontal rotator. A single crystal of **1** (0.48 mg) was mounted with its (100) face glued on an L-shaped Cu/Be support, in order to perform a rotation around the support's three orthogonal axes. The orientation of this crystal for magnetometry studies is described in Fig. S6.† Three series rotation data were collected under temperatures between 1.8 K and 5 K, at 10 000 Oe, and subsequently corrected for the diamagnetic contribution of the support and grease. The detailed experimental procedure has been described in the literature.[88]

Conflicts of interest

There are no conflicts of interest to declare.

Acknowledgements

P. K. would like to thank the Special Account of the National and Kapodistrian University of Athens for financial support. E. F. has been awarded a State Scholarship Foundation (IKY) fellowship, by the act "Support for Postdoctoral Researchers", from the operational program "Human Power Development, Education and Lifelong Learning" (6, 8, 9 priority axes), co-funded by the European Social Fund and the Greek State. V. P. would like to thank the Special Account of NCSR "Demokritos" for financial support concerning the operation of the X-ray facilities at INN through

the internal program entitled "Structural study and characterization of crystalline materials" (NCSR Demokritos, ELKE #10 813). S.-D. J. thanks the National Natural Science Foundation of China (21822301), the National Basic Research Program of China (2018YFA0306003) and the Beijing National Laboratory for Molecular Sciences (Y18G23), for funding. We are grateful to Dr Theodore Steriotis (INN, NCSR "Demokritos") for his contribution to the PXRD measurements, as well as to the Reviewers of the manuscript for their constructive comments.

References

1 R. Sessoli, D. Gatteschi, A. Caneschi and M. A. Novak, *Nature*, 1993, **365**, 141–143.
2 R. Sessoli, H. L. Tsai, A. R. Schake, S. Wang, J. B. Vincent, K. Folting, D. Gatteschi, G. Christou and D. N. Hendrickson, *J. Am. Chem. Soc.*, 1993, **115**, 1804–1816.
3 D. Gatteschi, L. Bogani, A. Cornia, M. Mannini, L. Sorace and R. Sessoli, *Solid State Sci.*, 2008, **10**, 1701–1709.
4 L. Bogani and W. Wernsdorfer, *Nat. Mater.*, 2008, **7**, 179–186.
5 J. W. Sharples and D. Collison, *Polyhedron*, 2013, **66**, 15–27.
6 R. Bagai and G. Christou, *Chem. Soc. Rev.*, 2009, **38**, 1011–1026.
7 G. Aromi and E. K. Brechin, *Struct. Bonding*, 2006, **122**, 1–67.
8 C. J. Milios and R. E. P. Winpenny, in *Molecular Nanomagnets and Related Phenomena*, ed. S. Gao, 2015, vol. 164, pp. 1–109.
9 C. J. Milios, A. Vinslava, W. Wernsdorfer, S. Moggach, S. Parsons, S. P. Perlepes, G. Christou and E. K. Brechin, *J. Am. Chem. Soc.*, 2007, **129**, 2754–2755.
10 A. M. Ako, I. J. Hewitt, V. Mereacre, R. Clerac, W. Wernsdorfer, C. E. Anson and A. K. Powell, *Angew. Chem., Int. Ed.*, 2006, **45**, 4926–4929.
11 J. Cirera, E. Ruiz, S. Alvarez, F. Neese and J. Kortus, *Chem. – Eur. J.*, 2009, **15**, 4078–4087.
12 F. Neese and D. A. Pantazis, *Faraday Discuss.*, 2010, **148**, 229–238.
13 D. N. Woodruff, R. E. P. Winpenny and R. A. Layfield, *Chem. Rev.*, 2013, **113**, 5110–5148.
14 Y. S. Meng, S.-D. Jiang, B. W. Wang and S. Gao, *Acc. Chem. Res.*, 2016, **49**, 2381–2389.
15 K. R. Meihaus and J. R. Long, *Dalton Trans.*, 2015, **44**, 2517–2528.
16 C. A. P. Goodwin, F. Ortu, D. Reta, N. F. Chilton and D. P. Mills, *Nature*, 2017, **548**, 439–442.
17 F. S. Guo, B. M. Day, Y. C. Chen, M. L. Tong, A. Mansikkamäki and R. A. Layfield, *Science*, 2018, **1062**, 1400–1403.
18 K. Randall McClain, C. A. Gould, K. Chakarawet, S. J. Teat, T. J. Groshens, J. R. Long and B. G. Harvey, *Chem. Sci.*, 2018, 8492–8503.
19 G. A. Craig and M. Murrie, *Chem. Soc. Rev.*, 2015, **44**, 2135–2147.
20 J. M. Frost, K. L. M. Harriman and M. Murugesu, *Chem. Sci.*, 2016, **7**, 2470–2491.
21 A. K. Bar, C. Pichon and J. P. Sutter, *Coord. Chem. Rev.*, 2016, **308**, 346–380.
22 M. Feng and M. L. Tong, *Chem. – Eur. J.*, 2018, **24**, 7574–7594.
23 S. Gomez-Coca, D. Aravena, R. Morales and E. Ruiz, *Coord. Chem. Rev.*, 2015, **289**, 379–392.
24 M. Atanasov, D. Aravena, E. Suturina, E. Bill, D. Maganas and F. Neese, *Coord. Chem. Rev.*, 2015, **289**, 177–214.
25 D. E. Freedman, W. H. Harman, T. D. Harris, G. J. Long, C. J. Chang and J. R. Long, *J. Am. Chem. Soc.*, 2010, **132**, 1224–1225.
26 M. Atzori, L. Tesi, E. Morra, M. Chiesa, L. Sorace and R. Sessoli, *J. Am. Chem. Soc.*, 2016, **138**, 2154–2157.
27 M. Atzori, S. Benci, E. Morra, L. Tesi, M. Chiesa, R. Torre, L. Sorace and R. Sessoli, *Inorg. Chem.*, 2018, **57**, 731–740.
28 C. Rajnák, J. Titiš, J. Moncol, R. Mičová and R. Boča, *Inorg. Chem.*, 2019, **58**, 991–994.
29 A. C. Benniston, S. Melnic, C. Turta, A. B. Arauzo, J. Bartolomé, E. Bartolomé, R. W. Harrington and M. R. Probert, *Dalton Trans.*, 2014, **43**, 13349–13357.
30 S. Q. Wu, Y. Miyazaki, M. Nakano, S. Q. Su, Z. S. Yao, H. Z. Kou and O. Sato, *Chem. – Eur. J.*, 2017, **23**, 10028–10033.
31 S. Tripathi, A. Dey, M. Shanmugam, R. S. Narayanan and V. Chandrsekhar, in *Topics in Organometallic Chemistry*, Springer, 2018, DOI: 10.1007/3418_2018_8.
32 D. Swenson, N. C. Baenziger and D. Coucouvanis, *J. Am. Chem. Soc.*, 1978, **100**, 1932–1934.
33 K. Fukui, N. Kojima, H. Ohya-Nishiguchi and N. Hirota, *Inorg. Chem.*, 1992, **31**, 1338–1344.
34 J. M. Zadrozny and J. R. Long, *J. Am. Chem. Soc.*, 2011, **133**, 20732–20734.
35 E. A. Suturina, D. Maganas, E. Bill, M. Atanasov and F. Neese, *Inorg. Chem.*, 2015, **54**, 9948–9961.
36 E. A. Suturina, J. Nehrkorn, J. M. Zadrozny, J. Liu, M. Atanasov, T. Weyhermuller, D. Maganas, S. Hill, A. Schnegg, E. Bill, J. R. Long and F. Neese, *Inorg. Chem.*, 2017, **56**, 3102–3118.
37 M. Craven, M. H. Nygaard, J. M. Zadrozny, J. R. Long and J. Overgaard, *Inorg. Chem.*, 2018, **57**, 6913–6920.
38 S. Sottini, G. Poneti, S. Ciattini, N. Levesanos, E. Ferentinos, J. Krzystek, L. Sorace and P. Kyritsis, *Inorg. Chem.*, 2016, **55**, 9537–9548.
39 X. N. Yao, M. W. Yang, J. Xiong, J. J. Liu, C. Gao, Y. S. Meng, S.-D. Jiang, B. W. Wang and S. Gao, *Inorg. Chem. Front.*, 2017, **4**, 701–705.
40 I. Haiduc, Dichalcogenoimidodiphosphinato Ligands in *Comprehensive Coordination Chemistry II: From Biology to Nanotechnology*, ed. J. A. McCleverty and T. J. Meyer, in Fundamentals, ed. A. B. P. Lever, Elsevier, Amsterdam, 2004, vol. 1, pp. 323–347.
41 J. Titiš and R. Boča, *Inorg. Chem.*, 2011, **50**, 11838–11845.
42 J. Vallejo, I. Castro, R. Ruiz-Garcia, J. Cano, M. Julve, F. Lloret, G. De Munno, W. Wernsdorfer and E. Pardo, *J. Am. Chem. Soc.*, 2012, **134**, 15704–15707.

43 A. Silvestru, D. Bilc, R. Rosler, J. E. Drake and I. Haiduc, *Inorg. Chim. Acta*, 2000, **305**, 106–110.
44 E. Ferentinos, D. Maganas, C. P. Raptopoulou, A. Terzis, V. Psycharis, N. Robertson and P. Kyritsis, *Dalton Trans.*, 2011, **40**, 169–180.
45 D. Maganas, J. Krzystek, E. Ferentinos, A. M. Whyte, N. Robertson, V. Psycharis, A. Terzis, F. Neese and P. Kyritsis, *Inorg. Chem.*, 2012, **51**, 7218–7231.
46 E. Ferentinos, C. P. Raptopoulou, V. Psycharis, A. Terzis, J. Krzystek and P. Kyritsis, *Polyhedron*, 2018, **151**, 177–184.
47 M. C. Aragoni, M. Arca, M. B. Carrea, A. Garau, F. A. Devillanova, F. Isaia, V. Lippolis, G. L. Abbati, F. Demartin, C. Silvestru, S. Demeshko and F. Meyer, *Eur. J. Inorg. Chem.*, 2007, 4607–4614.
48 N. Levesanos, A. Grigoropoulos, C. P. Raptopoulou, V. Psycharis and P. Kyritsis, *Inorg. Chem. Commun.*, 2013, **30**, 34–38.
49 F. D. Sokolov, D. A. Safin, N. G. Zabirov, L. N. Yamalieva, D. B. Krivolapov and I. A. Litvinov, *Mendeleev Commun.*, 2004, **14**, 51–52.
50 (*a*) L. M. Gilby and B. Piggott, *Polyhedron*, 1999, **18**, 1077–1082; (*b*) J. Novosad, M. Necas, J. Marek, P. Veltsistas, C. Papadimitriou, I. Haiduc, M. Watanabe and J. D. Woollins, *Inorg. Chim. Acta*, 1999, **290**, 256–260.
51 M. C. Aragoni, M. Arca, A. Garau, F. Isaia, V. Lippolis, G. L. Abbati and A. C. Fabretti, *Z. Anorg. Allg. Chem.*, 2000, **626**, 1454–1459.
52 A. M. Z. Slawin, M. B. Smith and J. D. Woollins, *J. Chem. Soc., Dalton Trans.*, 1996, 3659–3665.
53 M. Necas, M. R. S. Foreman, J. Marek, J. D. Woollins and J. Novosad, *New J. Chem.*, 2001, **25**, 1256–1263.
54 C. Silvestru and J. E. Drake, *Coord. Chem. Rev.*, 2001, **223**, 117–216.
55 D. Maganas, S. S. Staniland, A. Grigoropoulos, F. White, S. Parsons, N. Robertson, P. Kyritsis and G. Pneumatikakis, *Dalton Trans.*, 2006, 2301–2315.
56 D. V. Korchagin, A. V. Palii, E. A. Yureva, A. V. Akimov, E. Y. Misochko, G. V. Shilov, A. D. Talantsev, R. B. Morgunov, A. A. Shakin, S. M. Aldoshin and B. S. Tsukerblat, *Dalton Trans.*, 2017, **46**, 7540–7548.
57 R. Boča, C. Rajnák, J. Moncol, J. Titiš and D. Valigura, *Inorg. Chem.*, 2018, **57**, 14314–14321.
58 J. R. Pilbrow, *J. Magn. Reson.*, 1978, **31**, 479–490.
59 M. P. Shores, J. J. Sokol and J. R. Long, *J. Am. Chem. Soc.*, 2002, **124**, 2279–2292.
60 J. S. Griffith, *The Theory of Transition Metal Ions*, University Press, Cambridge, 1964.
61 O. Kahn, *Molecular Magnetism*, VCH Publishers, New York, 1993.
62 F. Lloret, M. Julve, J. Cano, R. Ruiz-García and E. Pardo, *Inorg. Chim. Acta*, 2008, **361**, 3432–3445.
63 N. F. Chilton, R. P. Anderson, L. D. Turner, A. Soncini and K. S. Murray, *J. Comput. Chem.*, 2013, **34**, 1164–1175.
64 D. Gatteschi, R. Sessoli and J. Villain, *Molecular Nanomagnets*, Oxford University Press, Oxford, U.K., 2006.
65 W. Wernsdorfer and R. Sessoli, *Science*, 1999, **284**, 133–135.
66 D. Maganas, S. Milikisyants, J. M. A. Rijnbeek, S. Sottini, N. Levesanos, P. Kyritsis and E. J. J. Groenen, *Inorg. Chem.*, 2010, **49**, 595–605.
67 J. M. Zadrozny, J. Telser and J. R. Long, *Polyhedron*, 2013, **64**, 209–217.
68 E. Ferentinos, S. Chatziefthimiou, A. K. Boudalis, M. Pissas, G. Mathies, P. Gast, E. J. J. Groenen, Y. Sanakis and P. Kyritsis, *Eur. J. Inorg. Chem.*, 2018, 713–721.
69 G. Mathies, S. D. Chatziefthimiou, D. Maganas, Y. Sanakis, S. Sottini, P. Kyritsis and E. J. J. Groenen, *J. Magn. Reson.*, 2012, **224**, 94–100.
70 S. M. Winter, S. Hill and R. T. Oakley, *J. Am. Chem. Soc.*, 2015, **137**, 3720–3730.
71 S. M. Winter, S. Datta, S. Hill and R. T. Oakley, *J. Am. Chem. Soc.*, 2011, **133**, 8126–8129.
72 J. Krzystek, J.-H. Park, M. W. Meisel, M. A. Hitchman, H. Stratemeier, L.-C. Brunel and J. Telser, *Inorg. Chem.*, 2002, **41**, 4478–4487.
73 H. I. Karunadasa, K. D. Arquero, L. A. Berben and J. R. Long, *Inorg. Chem.*, 2010, **49**, 4738–4740.
74 M. R. Saber and K. R. Dunbar, *Chem. Commun.*, 2014, 12266–12269.
75 L. Smolko, J. Cernak, J. Kuchar, C. Rajnak, J. Titis and R. Boca, *Eur. J. Inorg. Chem.*, 2017, 3080–3086.
76 S. Vaidya, S. K. Singh, P. Shukla, K. Ansari, G. Rajaraman and M. Shanmugam, *Chem. – Eur. J.*, 2017, **23**, 9546–9559.
77 S. Vaidya, A. Upadhyay, S. K. Singh, T. Gupta, S. Tewary, S. K. Langley, J. P. S. Walsh, K. S. Murray, G. Rajaraman and M. Shanmugam, *Chem. Commun.*, 2015, **51**, 3739–3742.
78 L. Smolko, J. Cernak, M. Dusek, J. Titis and R. Boca, *New J. Chem.*, 2016, **40**, 6593–6598.
79 A. K. Mondal, M. Sundararajan and S. Konar, *Dalton Trans.*, 2018, **47**, 3745–3754.
80 D. V. Korchagin, G. V. Shilov, S. M. Aldoshin, R. B. Morgunov, A. D. Talantsev and E. A. Yureva, *Polyhedron*, 2015, **102**, 147–151.
81 J. J. Liu, Y. S. Meng, I. Hlavicka, M. Orlita, S.-D. Jiang, B. W. Wang and S. Gao, *Dalton Trans.*, 2017, **46**, 7408–7411.
82 A. K. Mondal, T. Goswami, A. Misra and S. Konar, *Inorg. Chem.*, 2017, **56**, 6870–6878.
83 B. Drahos, R. Herchel and Z. Travnicek, *Inorg. Chem.*, 2017, **56**, 5076–5088.
84 A. Grigoropoulos, M. Pissas, P. Papatolis, V. Psycharis, P. Kyritsis and Y. Sanakis, *Inorg. Chem.*, 2013, **52**, 12869–12871.
85 *CrystalClear*, Rigaku/MSC Inc., The Woodlands, Texas, USA, 2005.
86 (*a*) G. M. Sheldrick, *Acta Crystallogr., Sect. A: Found. Crystallogr.*, 2008, **64**, 112–122; (*b*) G. M. Sheldrick, *Acta Crystallogr., Sect. C: Struct. Chem.*, 2015, **71**, 3–8.
87 *DIAMOND – Crystal and Molecular Structure Visualization, Ver. 3.1*, Crystal Impact, Rathausgasse 30, 53111, Bonn, Germany.
88 S.-D. Jiang, B. W. Wang and S. Gao, in *Molecular Nanomagnets and Related Phenomena*, ed. S. Gao, 2015, vol. 164, pp. 111–141.

